Ion-by-ion measurements of backward secondary electron emission of carbon foils under the impact of MeV H^+, H^0, H^-, and H_2^+ projectiles

A. Billebaud, M. Fallavier, R. Kirsch, J.-C. Poizat, J. Remillieux, and Z. Vidović
Institut de Physique Nucléaire de Lyon, IN2P3/CNRS, Université Claude Bernard 43, Boulevard du 11 Novembre 1918, F-69622 Villeurbanne Cedex, France

(Received 30 July 1996)

We have experimentally studied the backward electron emission from solid carbon bombarded by H^+, H^0, H^-, and H_2^+ projectiles at MeV energies. We used a coincidence ion-by-ion technique that allows us to obtain not only the average electron yields but also the emission statistics. The comparison of energy dependences of electron emission due to H^+ and H^0 projectiles helps to specify the role of the incident electron of H^0. For H^- and H_2^+, the equality of electron yields above 500 keV/u supports the idea that backward emission is due to distant collisions. [S1050-2947(97)06002-2]

PACS number(s): 34.50.Bw, 79.20.Rf

Kinetic electron emission from solid surfaces under impact of various hydrogen projectiles has been studied by many groups in the recent years. In the case of incident protons, in an energy range where kinetic emission is dominant (above a few keV), the mean number of electrons emitted per incident particle, γ, has been shown to be proportional to the electronic stopping power of the medium, S_e, through the so-called material parameter Λ: $\gamma = \Lambda S_e$ [1].

In the case of composite hydrogen projectiles such as H^0, H^-, H_2^+, H_3^+, or H_n^+ which have all been experimentally used at least once for such studies, a full understanding is much more difficult to reach: even if electron emission is still related to the slowing down process of the projectile components, it is complicated both by the collective aspects of the interaction of the composite projectile with the target electrons, and by the rapid evolution of the projectile in the solid (ionization, fragmentation). In particular we have recently studied the projectile velocity dependence of the backward electron yield of a carbon surface bombarded by H_n^+ cluster ions. If expressed in units of the total yield of n independent protons of the same velocity, the yield for large ($n > 7$) H_n^+ projectiles is equal to 0.5 at 40 keV/u, then increases with velocity, and seems to reach unity around 200 keV/u [2]. Moreover, measurements performed with incident electrons, protons, H_2^+ and H_3^+ ions in the velocity range of a few MeV/u have shown that the electron yields induced by H_2^+ and H_3^+ impacts are smaller than the summed yields of the components [3]. It can be thought that the collective effects are partly due to the mutual screening of projectile electrons and protons.

In order to get more insight into these effects, which have been experimentally observed mainly by current measurements, we have used an event-by-event technique that allows us to count secondary electrons emitted by each incident projectile. This technique, used by several groups under various forms [4–6], presents many decisive advantages over electrical measurements. It can be used with very low beam intensities, provides not only the mean yield, but also the emission statistics. Furthermore, if a thin target is used, the electron emission from both entrance and emergence sides can be measured in coincidence with the transmitted projectile (or transmitted fragments if the incident projectile is a molecule), which allows the elimination of background electron emission (due to cold emission), and also the restriction of electron emission measurements to projectiles that have interacted with the target in a particular way, a property that will not be used in the present report.

Our experimental equipment has been designed to count electrons emitted by both sides of thin solid targets tilted at 45° to the beam direction, and maintained at a negative potential $-V_0$ (V_0 being typically 20 kV). Two grounded silicon detectors face the entrance and the emergence side of the target, respectively. If n electrons are emitted by a given surface, the electron detector delivers a signal corresponding to the energy neV_0. We used a carbon target of thickness 1200 Å.

Incident and emergent particle trajectories may be affected by the strong electric field set in the target area. A first pair of parallel plates located in front of the target produces a transverse electric field that maintains the impact location of the tightly collimated incident beam (~ 50 μm in diameter) on the target when it is brought to potential $-V_0$. For the same reason a second pair of plates located downstream from the target directs charged transmitted particles onto the silicon detector located on the beam line and used to trigger electron counting.

Our goal was to compare electron emission from carbon surfaces bombarded by H^+, H^0, H^-, and H_2^+ projectiles of the same velocity. H^+ and H_2^+ beams were delivered by the 2.5-MV Van de Graaff accelerator of our Institute, and the H^0 secondary beam was obtained by electron capture in the residual gas of the upper section of the beam line. The H^- secondary beam was obtained from the breakup of H_3^+ ions in the residual gas between the accelerator and the analyzing magnet.

In Fig. 1 we show the energy spectra delivered by the back Si detector for incident 1.5-MeV protons (a) and neutral hydrogen atoms (b). The electron number is indicated for each peak. The peak labeled ''0'' corresponds to the measurement of the detector noise when no electron is emitted in coincidence with a transmitted particle. Of course, only its area has a physical meaning. The electron multiplicity distri-

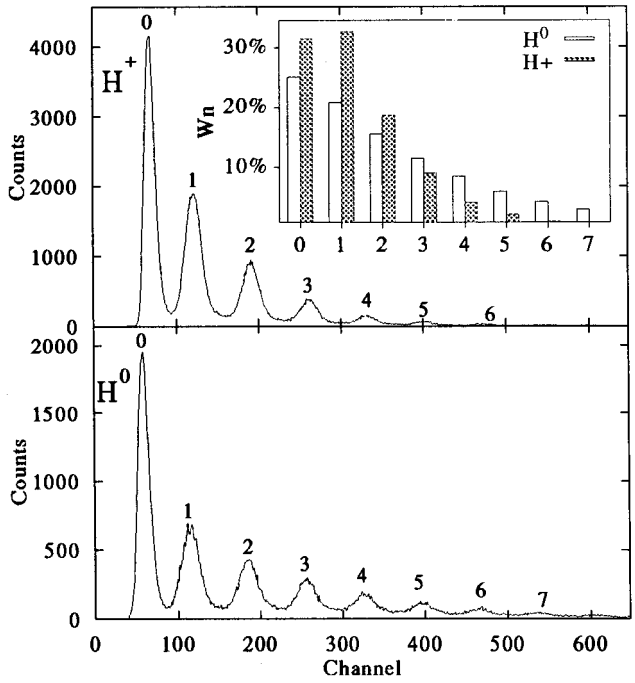

FIG. 1. Energy spectra of backward secondary electrons detected for 1.5-MeV H^+ and H^0 projectiles incident on a carbon foil tilted at 45°. The electron number corresponding to each peak is indicated. The emission statistics deduced from the fits are given as an inset.

bution has been deduced from a fitting procedure that takes into account not only the energy resolution of the detector ($\sim$6 keV), but also the probability of each electron to be backscattered out of the detector ($\sim$17%) and then to deposit in the detector a reduced amount of energy ($\sim 0.6eV_0$) [7]. The simulated spectra are not shown because they are very close to the experimental ones. The resulting normalized distributions W_n are given as an inset in Fig. 1. From W_n values one deduces first the average yields (with a 5% accuracy), 1.26 for protons and 2.26 for H^0. Of course the incident electron of H^0 is seen to contribute to the process since the yield is higher for H^0 than for H^+, but one may wonder whether the two components of H^0 participate independently. If they do the comparison of the two normalized distributions $W_n(H^+)$ and $W_n(H^0)$, for H^+ and H^0, respectively, must yield the distribution $W_n(e^-)$ that would be observed for incident electrons of the same velocity: it is straightforward to show that the $W_n(e^-)$ values can be calculated step by step using the following expression:

$$W_n(e^-) = \frac{W_n(H^0) - \sum_{i=1}^{n} W_i(H^+) W_{n-i}(e^-)}{W_0(H^+)}, \qquad (1)$$

the first term to be calculated being

$$W_0(e^-) = \frac{W_0(H^0)}{W_0(H^+)}. \qquad (2)$$

Trying to follow the procedure leads to a complete failure since the second calculated term $W_1(e^-)$ is found negative,

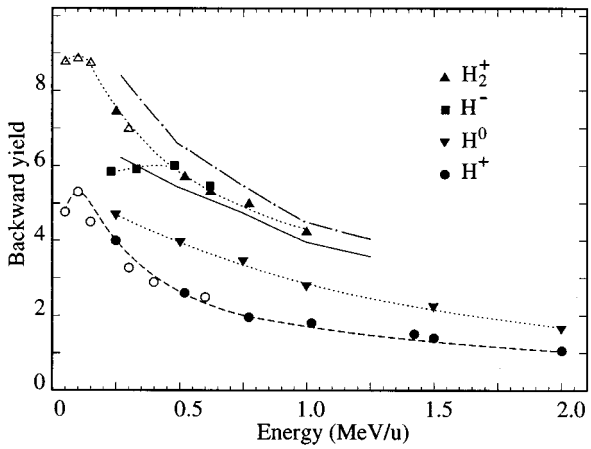

FIG. 2. Energy dependence of the backward electron emission yields due to impacts of H^+, H^0, H^-, and $H_2{}^+$ projectiles, respectively, on a carbon foil tilted at 45°. The dashed line represents the energy dependence of the proton energy loss (normalized to coincide with the maximum electron yield). Open symbols correspond to yields obtained by the current measurement technique in previous experiments. The dotted lines only guide the eye. Calculated yields (see text) are given for H^- (full line) and for $H_2{}^+$ (dash-dotted line).

and this is not due to poor statistics. The same feature was obtained for all incident energies. This is the clear demonstration that the electron emission due to H^0 is not just the addition of the electron emission due to its two components.

In Fig. 2 we show the energy dependence of backward electron emission yields from the same carbon target bombarded by H^+, H^0, H^-, and $H_2{}^+$ ions, respectively. As stated above, the yields induced by protons are seen to follow the behavior of the electronic stopping power of carbon which is represented by a dashed line (and normalized to the maximum yield). The yields obtained with our setup show also a good agreement with the ones we had obtained by current measurements (after cosine correction for the incidence angle). Over the whole energy range of our measurements (250 keV/u to 2 MeV/u) the electron emission yield due to H^0 impacts, $\gamma_m(H^0)$, is larger than the yield due to protons. The ratio of these yields, shown in Fig. 3, is found constant around 1.6 above 500 keV/u, a value in agreement with the one measured at 1.2 MeV/u by Kroneberger *et al* [8]. Below 500 keV/u the ratio decreases, and would probably be smaller than unity below 150 keV/u. Indeed, this has been observed in the energy range 2–16 keV/u [9].

In order to compare secondary electron emission by H^+ and H^0 projectiles, it is convenient to consider the parameter λ_{se}, the secondary electron mean escape depth, which has been introduced in theoretical descriptions derived from the semiempirical model of Sternglass [10]. This is especially useful in our case since it gives the order of magnitude of the depth over which the charge state of the incident projectile must be considered in detail. As usually admitted we consider that λ_{se} is independent of the projectile and of its velocity, like the mean energy of ''internal'' secondary electrons.

In our velocity range the electron loss cross section of H^0 projectiles is much larger than the cross section for elec-

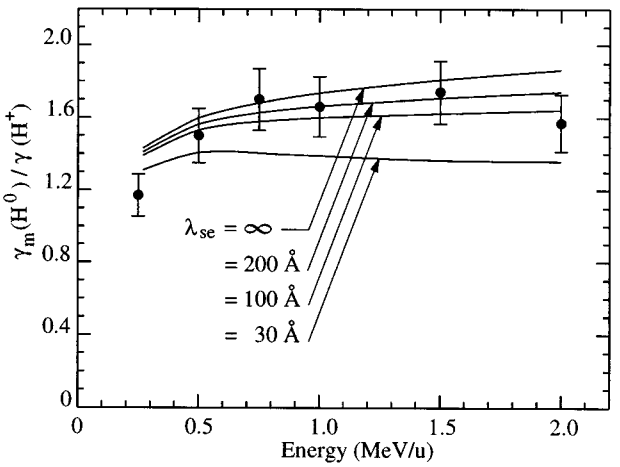

FIG. 3. Comparison of backward experimental and calculated ratios $\gamma_m(H^0)/\gamma(H^+)$ as a function of the incident energy.

tron capture by protons, that can thus be neglected. The mean free path length λ_0 for H^0 projectile has been found to be proportional to the projectile velocity [11,12]. Clearly the number of secondary electrons emitted for an incident H^0 projectile must depend on the depth x at which it has been ionized. Before ionization, the electron production may be thought to be reduced (with respect to the proton case) because the bound electron is not allowed to participate but just screens the proton. After ionization, the proton and the freed electron are assumed to contribute independently to the electron production, a reasonable and necessary approximation. From this above description we deduce how to calculate the velocity dependence of the ratio $\gamma_m(H^0)/\gamma(H^+)$, as undertaken many years ago by Ghosh and Khare [13].

The number of backward secondary electrons due to a given projectile and coming from a depth contained between x and $x+dx$ (for a target tilted at 45°) is

$$d\gamma = \frac{\gamma}{\sqrt{2}\lambda_{se}} e^{-x/\sqrt{2}\lambda_{se}} dx, \tag{3}$$

where $\exp(-x/\sqrt{2}\lambda_{se})$ represents the attenuation of the secondary electron escape probability. The integration of this expression over the thickness of the target gives the measured yield γ. In the case of a H^0 projectile, the measured number $d\gamma_m(H^0)$ of electrons coming from dx can be expressed as the sum of the contribution of a H^0 projectile in its frozen charge state, $d\gamma(H^0)$, and the respective contributions of a proton, $d\gamma(H^+)$ and of an electron, $d\gamma(e^-)$, each of the three terms being weighted by the fractions of neutrals and ionized projectiles at the depth x. It is given by

$$d\gamma_m(H^0) = \Phi_0(x) d\gamma(H^0) + [1-\Phi_0(x)] d\gamma(H^+) + [1-\Phi_0(x)] d\gamma(e^-). \tag{4}$$

The neutral hydrogen fraction $\Phi_0(x)$ is given by $\Phi_0(x) = \exp(-x/\lambda_0)$ [one assumes $\Phi_0(\infty) \simeq 0$], where λ_0 is deduced from the electron loss cross sections for carbon [12] (with the number of target atoms per unit volume $N = 8.28 \times 10^{22}$ atoms/cm^3 for evaporated carbon foils), and $d\gamma(H^0)$ and $d\gamma(H^+)$ being derived from Eq. (3). Before integrating this equation it must be specified that the integrated yield $\gamma(e^-)$ is due not only to secondary electrons resulting from energy deposition by the incident electron, but may also result from backscattering of incident electrons on target atoms. Its differential form can be written

$$d\gamma(e^-) = d\gamma'(e^-) + \varepsilon(x) dx, \tag{5}$$

where $d\gamma'(e^-)$ represents the true secondary electrons and $\varepsilon(x)dx$ the backscattered fraction. While $d\gamma'(e^-)$ is given by Eq. (3), the function $\varepsilon(x)$ is not readily available, but its integral from zero to infinity, $\eta(e^-)$, the backscattered fraction for a thick target, has been measured by Hölzl and Jacobi [14]. In the following we will assume that $\eta(e^-)$ is the same wherever the electron is lost by the projectile, since the ranges of backscattered electrons are much larger than λ_0. The measured yield $\gamma_m(H^0)$ can then be calculated by integrating Eq. (4) over the whole target thickness (much larger than λ_{se} and λ_0), and can be written [when expressed in units of $\gamma(H^+)$]:

$$\frac{\gamma_m(H^0)}{\gamma(H^+)} = \frac{\lambda_0}{\lambda_0+\sqrt{2}\lambda_{se}} \frac{\gamma(H^0)}{\gamma(H^+)} + \left(1 - \frac{\lambda_0}{\lambda_0+\sqrt{2}\lambda_{se}}\right) \times \left(1 + \frac{\gamma'(e^-)}{\gamma(H^+)}\right) + \frac{\eta(e^-)}{\gamma(H^+)}. \tag{6}$$

In order to calculate the ratio $\gamma(H^0)/\gamma(H^+)$ we consider that the secondary electron yield of a given projectile in a frozen charge state is proportional to its energy loss rate: $\gamma(H^+) = \Lambda S_e(H^+)$ and $\gamma(H^0) = \Lambda S_e(H^0)$, where Λ (depending only on the material) is the same for both projectiles. The ratio $\gamma(H^0)/\gamma(H^+)$ will consequently vary with the velocity like $S_e(H^0)/S_e(H^+)$, $S_e(H^0)$ being derived from calculations made by Kaneko [15]. As for the ratio $\gamma'(e^-)/\gamma(H^+)$, it can then be evaluated in a similar way [assuming $\gamma'(e^-) = \Lambda S_e(e^-)$] from stopping power Bethe-Bloch formulas, that give a ratio varying from 0.25 at 0.2 MeV/u to a saturation value of 0.7 at 2 MeV/u. This calculation is also in good agreement with the ratio obtained from the $\gamma'(e^-)$ measurements of Ref. [14] and from our present experimental values of $\gamma(H^+)$. Finally, one can write

$$\frac{\gamma_m(H^0)}{\gamma(H^+)} = \frac{\lambda_0}{\lambda_0+\sqrt{2}\lambda_{se}} \frac{S_e(H^0)}{S_e(H^+)} + \left(1 - \frac{\lambda_0}{\lambda_0+\sqrt{2}\lambda_{se}}\right) \times \left(1 + \frac{S_e(e^-)}{S_e(H^+)}\right) + \frac{\eta(e^-)}{\gamma(H^+)}. \tag{7}$$

The fraction $\eta(e^-)$ given in Ref. [14] is found nearly constant at the value 0.18 (after correction for our incidence angle) over the energy range of our experiments. The results of these calculations for λ_{se} values 30, 100, and 200 Å, and infinity, respectively, are shown in Fig. 3 along with our experimental values of the ratio $\gamma_m(H^0)/\gamma(H^+)$. The best agreement is reached for $\gamma_{se} = 100$ Å. However, it is clear from Fig. 3 that the ratio depends only weakly upon λ_{se} when λ_{se} is much larger than λ_0 (the limiting value of $\gamma_m(H^0)$ is $[\gamma(e^-)+\gamma(H^+)]$, the sum of the yields for independent electrons and protons). This is why λ_{se} cannot be determined very accurately. However, this value is of the order of magnitude of the one found by Ghosh and Khare to fit experimental data [13], but significantly larger than the

values currently used after Sternglass corresponding rather to electron inelastic mean free paths.

It remains that, basically, the electron yield due to H^0 projectiles is less than the summed yields of independent electrons and protons because significant secondary electron production only starts at the mean depth λ_0.

In Fig. 2 are also shown the energy dependences of electron yields induced by H^- and $H_2{}^+$ projectiles. Whereas the yield is lower for H^- than for $H_2{}^+$ below 500 keV/u, the two curves are observed to merge at this energy, up to 750 keV/u, the maximum H^- energy available. In this last velocity range, not only the electron yields are equal for a given velocity, but also the distributions of the number of emitted electrons are similar. This surprising finding may qualitatively be understood in the following way: H^- and $H_2{}^+$ ions correspond with each other by exchange of protons and electrons because for these ions the relative distances between components are quite comparable. Then the above result suggests that, above a given velocity, backward electron emission yields are the same for protons and electrons. Concerning the charge this is not surprising since slowing down and secondary electron emission depend essentially upon the square of the projectile charge. As for the mass difference we have seen above that $S_e(e^-)$ is significantly smaller than $S_e(H^+)$ in this energy range, which is due to the fact that energy transfers to target electrons in close collisions are much smaller for incident electrons than for protons of the same velocity. We are then lead to conclude that backward electron emission is mostly due to distant collisions. This is probably the first experimental result that reveals this property of backward electron emission (measurements with incident electrons and protons [3] have been performed on materials heavier than carbon and seem to indicate that electrons and protons should give nearly equal backward yields for low Z materials as carbon in the MeV/u energy range). This had to be expected since δ electrons resulting from small impact parameter collisions are emitted in the forward direction. Indeed it had been predicted by Sternglass [10] for light targets.

However, it must be said that the small contribution $\eta(e^-)$ of backscattered electrons has not been included in the above discussion. Moreover, the equality of secondary electron yields observed here is obtained for a carbon target. For higher Z targets the situation could be different both because $\eta(e^-)$ should be larger and because close collisions should come into play through backscattering of δ electrons on target nuclei.

In order to fit H^- and $H_2{}^+$ electron yields, a similar attempt to that undertaken to reconstruct the H^0 electron yield can be made. Assuming that a H^- projectile splits rapidly into a H^0 and an electron (a reasonable assumption in view of its short collisional lifetime [16]), we may neglect its contribution in its frozen charge state. Then the $\gamma(H^-)$ electron yield can be expressed as the sum of the yields due to the independent incident electron and the neutral hydrogen atom. The reconstructed yield using the $\gamma(e^-)$ values discussed above and our experimental $\gamma_m(H^0)$ values is shown by a full line in Fig. 2. Even if the fit values are close to the experimental ones, it is quite probable that this procedure would give too large fitted values below 250 keV.

As for the $H_2{}^+$ case, a first similar and rough approach can be made that leads to express $\gamma(H_2{}^+)$ as the sum of independent projectiles H^+ and H^0. The result, also shown in Fig. 2 as a dash dotted line, is seen to overestimate $\gamma(H_2{}^+)$ below750 keV/u, but tends to agree with experiment and with the $\gamma(H^-)$ fit above this energy. This last feature is not surprising since electron yields due to electrons and protons have been seen earlier to be nearly equal in this energy range. Now, if we try to calculate $\gamma(H_2{}^+)$ by taking into account the $H_2{}^+$ collisional lifetime [16] and assuming that it always splits into H^+ and H^0 (which is not true, as it can also split directly into two H^+ and one electron), we obtain slightly lower yields, which still do not fit our experimental data at low energies.

We do not understand why we cannot fit our $H_2{}^+$ data at low energy (and also the H^- data; see above). However, we may say the following: what would be the backward electron emission under impact of two nearby particles with charges of the same sign, for instance, two protons at the distance of 1 Å? It probably would not be equal to twice the yield of a single proton, at least because each target electron interacts with the two projectiles simultaneously (for the same reason the energy loss rate would be also affected, which has been observed previously with incident hydrogen clusters). However, it has been also observed [2] that the forward electron emission of emergent protons resulting from the dissociation of $H_n{}^+$ clusters in a thin carbon foil is lower than expected from a simple addition of yields. This happens for relative separation distances of several angströms, and thus cannot be explained by changes in the energy loss rate. This effect may probably lower the backward electron emission, but cannot be studied separately because of the major role of electrons in incident molecules or clusters. However, we have simultaneously studied the forward electron emission and the results, presently under analysis, will be published in the near future, along with the detailed analysis of the emission statistics.

[1] D. Hasselkamp, H. Rothard, K. O. Groeneveld, J. Kemmler, P. Varga, and H. Winter, in *Particle Induced Electron Emission II*, edited by G. Höhler and E. A. Niekisch, Springer Tracts in Modern Physics Vol. 123 (Springer, Berlin, 1991).

[2] A. Billebaud, D. Dauvergne, M. Fallavier, R. Kirsch, J.-C. Poizat, J. Remillieux, H. Rothard, and J.-P. Thomas, Nucl. Instrum. Methods Phys. Res. Sect. B **112**, 79 (1996).

[3] D. M. Suszcynsky and J. E. Borovsky, Nucl. Instrum. Methods Phys. Res. Sect. B **53**, 255 (1991).

[4] Y. Yamazaki and K. Kuroki, Nucl. Instrum. Methods Phys. Res. Sect. A **262**, 118 (1987).

[5] G. Lakits, F. Aumayr, and H. Winter, Rev. Sci. Instrum. **60**, 3151 (1989).

[6] O. Benka, E. Steinbauer, O. Bolik, and T. Fink, Nucl. Instrum.

Methods Phys. Res. Sect. B **93**, 156 (1994).
[7] The procedure for fitting the electron energy spectra including the contribution of backscattered electrons is similar to the method detailed by Lakits *et al.* [5].
[8] K. Kroneberger, A. Clouvas, G. Schlüssler, P. Koschar, J. Kemmler, H. Rothard, C. Biedermann, O. Heil, M. Burkhard, and K. O. Groeneveld, Nucl. Instrum. Methods Phys. Res. Sect. B **29**, 621 (1988).
[9] G. Lakits, F. Aumayr, and H. Winter, Europhys. Lett. **10**, 679 (1989).
[10] E. J. Sternglass, Phys. Rev. **108**, 1 (1957).
[11] M. J. Gaillard, J.-C. Poizat, A. Ratkowski, J. Remillieux, and M. Auzas, Phys. Rev. A **16**, 2323 (1977).
[12] L. H. Toburen, M. Y. Nakai, and R. A. Langley, Phys. Rev. **171**, 114 (1968).
[13] S. N. Ghosh and S. P. Khare, Phys. Rev. **125**, 1254 (1962).
[14] J. Hölzl and K. Jacobi, Surf. Sci. **14**, 351 (1969).
[15] T. Kaneko, Phys. Rev. A **43**, 4780 (1991).
[16] N. Cue, N. V. de Castro-Faria, M. J. Gaillard, J.-C. Poizat, and J. Remillieux, Nucl. Instrum. Methods **170**, 67 (1980).